



HAL
open science

Pulse compression down to 20 fs using a photonic crystal fiber seeded by a diode-pumped Yb:SYS laser at 1070 nm

Frédéric Druon, Patrick Georges

► To cite this version:

Frédéric Druon, Patrick Georges. Pulse compression down to 20 fs using a photonic crystal fiber seeded by a diode-pumped Yb:SYS laser at 1070 nm. *Optics Express*, 2004, 12 (15), pp.3383-3396. hal-00686985

HAL Id: hal-00686985

<https://hal-iogs.archives-ouvertes.fr/hal-00686985>

Submitted on 11 Apr 2012

HAL is a multi-disciplinary open access archive for the deposit and dissemination of scientific research documents, whether they are published or not. The documents may come from teaching and research institutions in France or abroad, or from public or private research centers.

L'archive ouverte pluridisciplinaire **HAL**, est destinée au dépôt et à la diffusion de documents scientifiques de niveau recherche, publiés ou non, émanant des établissements d'enseignement et de recherche français ou étrangers, des laboratoires publics ou privés.

Pulse-compression down to 20 fs using a photonic crystal fiber seeded by a diode-pumped Yb:SYS laser at 1070 nm

Frédéric Druon and Patrick Georges

Laboratoire Charles Fabry de l'Institut d'Optique du CNRS et de l'Université Paris-Sud, Centre Universitaire,
Bat 503, 91403 Orsay Cedex, France Phone: (33) 1 69 35 88 52, Fax: (33) 1 69 35 88 07,
frederic.druon@iota.u-psud.fr

<http://www.elsa-laser.com>

Abstract: We studied experimentally and theoretically the pulse compression using a zero-dispersion photonic crystal fiber in order to optimize the pulse duration and pulse shape. 20.3-fs pulses centered at 1070 nm have been produced using a diode-pumped system based on Yb:SYS crystal. The limitations such as pre-pulse amplitude or solitonic fission have also been studied.

©2004 Optical Society of America

OCIS codes: 320.7140 Ultrafast processes in fibers, 320.5520 Pulse compression, 060.5530 Pulse propagation and solitons.

References and links

1. E. Innerhofer, T. Sudmeyer, F. Brunner, R. Hring, A. Aschwanden, R. Paschotta, C. Honninger, M. Kumkar, U. Keller, "60-W average power in 810-fs pulses from a thin-disk YbYAG laser," *Opt. Lett.* **28** 367 (2003).
2. M.E. Fermann, A. Galvanauskas, G. Sucha, D. Harter, "Ultrafast pulse sources based on multi-mode optical fibers," *Appl. Phys. B* **65**, 259-275 (1997).
3. C. Hönninger, R. Paschotta, M. Graf, F. Morier-Genoud, G. Zhang, M. Moser, S. Biswal, J. Nees, A. Braun, G. Mourou, I. Johannsen, A. Giesen, W. Seeber, U. Keller, "Ultrafast ytterbium-doped bulk laser amplifiers," *Appl. Phys. B*, **69**, 3-17 (1999).
4. F. Druon, F. Balembois, P. Georges, "Laser crystals for the production of ultra-short laser pulses," *Ann. Chim. – Sci. Mat. (Ed. Elsevier SAS)* **28**, 47-72 (2003).
5. C. M.J. Gander, R. McBride, J.D.C. Jones, D. Mogilevstev, T.A. Birks, J.C. Knight, P.St.J. Russel, "Experimental measurement of group velocity dispersion in photonic crystal fiber," *Electron. Lett.* **35**, 63-64 (1999).
6. B.R. Washburn, S.E. Ralph, P.A. Lacourt, J.M. Dudley, W.T. Rhodes, R.S. Windeler, S. Coen, "Tunable near-infrared femtosecond soliton generation in photonic crystal fibres," *Electron. Lett.* **37**, 1510-1512 (2001).
7. I.G. Cormack, D.T. Reid, W.J. Wadsworth, J.C. Knight, P.St.J. Russel, "Observation of soliton self-frequency shift in photonic crystal fibre," *Electron. Lett.* **38**, 167-168 (2002).
8. F. Druon, N. Sanner, G. Lucas-Leclin, P. Georges, K.P. Hansen, A. Peterson, "Self-Compression and Raman Soliton Generation in a Photonic Crystal Fiber of 100-fs Pulses Produced by a Diode-Pumped Yb-Doped Oscillator," *Appl. Opt.* **42**, 6768 (2003).
9. J.H.V. Price, K. Furasawa, T.M. Monro, L. Lefort, D.J. Richardson, "Tunable, femtosecond pulse source operating in the range 1.06–1.33 μm based on an Yb³⁺-doped holey fiber amplifier," *J. Opt. Soc. Am. B* **19**, 1286-94 (2002).
10. T. Sudmeyer, F. Brunner, E. Innerhofer, R. Paschotta, U. Keller, K. Furasawa, J. Bagget, T. Monro, D. Richardson, "Nonlinear femtosecond pulse compression at high average power levels by use of a large-mode-area holey fiber," *Opt. Lett.* **28** 1951-1953 (2003).
11. G. McConnell, E. Riis, "Ultrashort pulse compression using photonic crystal fiber," *Appl. Phys. B* 557-563 (2004)
12. F. Druon, S. Chénais, P. Raybaut, F. Balembois, P. Georges, R. Gaumé, P.H. Haumesser, B. Viana, D. Vivien, S. Dhellemmes, V. Ortiz, C. Larat, "Apatite-structure crystal, Yb³⁺:SrY₄(SiO₄)₃O, for the development of diode-pumped femtosecond lasers," *Opt. Lett.* **27** 1914-1916 (2002).
13. <http://www.crystal-fibre.com/>

14. R. L. Fork , O. E. Martinez , and J. P. Gordon, "Negative dispersion using pairs of prisms," *Opt. Lett.* **9**, 150-152 (1984).
 15. G. P. Agrawal, *Nonlinear fiber optics*, (Academic press, Inc. 1994).
 16. J.W. Nicholson, J. Jasapara, W. Rudolph, F.G. Omenetto, A.J. Taylor, "Full-f field characterization of femtosecond pulses by spectrum and cross-correlation measurements," *Opt. Lett.* 1774-76 (1999) and 138 (2000).
 17. R. Trebino, K. W. DeLong, D. N. Fittinghoff, J. N. Sweetser, M. A. Krumbugel, B. A. Richman, and D. J. Kane, "Measuring ultrashort laser pulses in the time-frequency domain using frequency-resolved optical gating," *Rev. Sci. Instrum.* **68**, 3277-3295 (1997).
 18. J. M. Dudley, X. Gu, L. Xu, M. Kimmel, E. Zeek, P. O'Shea, and R. Trebino, S. Coen, R. S. Windeler, "Cross-correlation frequency resolved optical gating analysis of broadband continuum generation in photonic crystal fiber: simulations and experiments," *Opt. Express* **10**, 1215-1221 (2002).
 19. K.M. Hilligsøe, T. V. Andersen, H. N. Paulsen, C. K. Nielsen, K. Mølmer, S. Keiding, R. Kristiansen and K. P. Hansen "Supercontinuum generation in a photonic crystal fiber with two zero dispersion wavelengths," *Opt. Express* **12** . 6, 1045-55 (2004).
 20. A. V. Husakou and J. Herrmann, "Supercontinuum Generation of Higher-Order Solitons by Fission in Photonic Crystal Fibers," *Phys. Rev. Lett.* **87**, 203901 (2001).
 21. J. Dudley, S. Coen , "Coherence properties of supercontinuum spectra generated in photonic crystal and tapered optical fibers," *Opt. Lett.* **27**, 1180-82 (2002). J. Dudley, S. Coen , "Coherence properties of supercontinuum spectra generated in photonic crystal and tapered optical fibers," *Opt. Lett.* **27**, 1180-82 (2002).
 22. X. Gu, M. Kimmel, A. P. Shreenath, R. Trebino, J. M. Dudley, S. Coen, R. S. Windeler, "Experimental studies of the coherence of microstructure-fiber supercontinuum," *Opt. Express* **11**, 2997-2703 (2003).
 23. W. J. Tomlinson, R. H. Stolen, C. V. Shank, "Compression of optical pulses chirped by self-phase modulation in fibers," *J. Opt. Soc. Am. B* **1** 139-149 (1984).
-

1. Introduction

Within the past few years, diode-pumped femtosecond laser systems have lead to a very strong interest in various scientific and engineering fields. Among them, systems based on Yb-doped crystals have allowed significant breakthroughs in terms of efficiency, compactness and reliability [1-4]. However, the pulse duration of these lasers is usually limited around 100 fs [4] mainly due to the emission bandwidth of the Yb-doped materials. Alternatively, photonic crystal fibers (PCF) have allowed a revolutionary breakthrough in non-linear optics. Actually, an intense interest has arisen due to the novel PCF dispersion properties and the opportunity for propagation within a tightly confined fundamental spatial mode [5]. Very efficient continuum generation, pulse compression and even solitonic tunability have been demonstrated using PCF. And it has been shown that the temporal dynamics which are observed during femtosecond pulse propagation in PCF strongly depend on the input pulse power and the proximity of the input wavelength to the fiber zero dispersion wavelength (ZDW) [6,7]. On the first hand, the use of fibers with negative group velocity dispersion (GVD) at the laser emission allows to obtain straightforward self-compression and easily tunable sources [8-10]. In fact, we previously demonstrated the self-compression of 1- μ m pulses from 110 fs to 75 fs using a fiber with a ZDW at 950 nm [8]. However, solitonic fission (due to the combined effects of stimulated Raman scattering (SRS) and dispersion) rapidly occurred in negative GVD fibers, avoiding then the generation of very broad spectra and important compression. On the other hand, very large compression factor have been demonstrated using a PCF with a ZDW at the laser emission and an additional prism compressor [10-11]. With this method, very efficient pulse compression from 810 fs to 33 fs has been obtained with a high average power [10]. Nevertheless, involving shorter pulsed oscillators is an interesting way out to achieve shorter pulse generation with photonic-crystal-fiber compression. In fact, new simple and efficient laser systems emitting around 1 μ m and producing ultra-short-pulses are interesting and promising in the fields of ultra-fast phenomena or athermal micromachining. In this paper, we are presenting an experimental and theoretical study of ultrashort pulse compression using a zero-dispersion photonic crystal fiber with the purpose of producing the shortest pulses with respect of the pulse shape quality. After the description of the experimental setup, the optimal results obtained with this system will be

presented and compared with the theory, and finally we will discuss the limitation of such a system taking into account the pre-pulse amplitude and solitonic fission.

2. Experimental setup

In order to have a very efficient system in the 100-fs-duration range, the experiment (Fig.1) was performed with a diode-pumped oscillator based on an Yb:SYS crystal [12]. This oscillator produced 110-fs pulses at a repetition rate of 98 MHz and with an average power of 400 mW (≈ 37 kW peak power). The spectral bandwidth of the pulses was 13 nm centered at 1070 nm, corresponding to a time-bandwidth product (TBP) of 0.37.

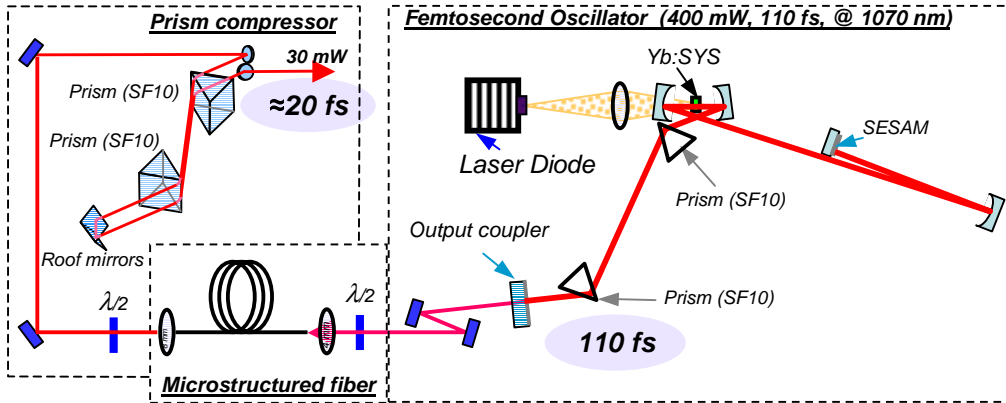


Fig. 1. Experimental setup.

Concerning the injection in the fiber, the incident polarization and the coupled power were controlled respectively by a half-wave plate and 2 mirrors. Under these conditions, the injected power in the fiber was continuously adjusted without modifying the performances of the oscillator. Moreover, the extremely good stability of the modelocked Yb:SYS laser allows us to avoid the use of an optical isolator since no instability of the oscillator was observed due to feedbacks from the fiber. The beam is injected in the fiber using a 4-mm-focal-length aspherical lens, leading to a maximum coupling efficiency around 30 % (113 mW at the output of the fiber). The output beam is re-collimated at the end of the fiber by an 8-mm-focal-length aspherical lens. The fiber (from Crystal Fiber[13]) has its zero dispersion wavelength centered at 1065 nm. It is 20-cm long and has a core size of 5 ± 0.2 μm . At the output of the fiber the beam profile is perfectly single-mode, and the polarization is nearly linear. The post-compression of the pulses are made using a prism compressor[14]. This compressor uses two SF10 prisms double-passed and roof mirrors acting in the vertical plan. The distance between the two prisms can be adjusted between 10 and 60 cm in order to optimize the pulse compression. The spectral characterization of the pulses is obtained with an optical spectrum analyzer, and the temporal characterization is achieved by a second order autocorrelator used in both configurations: interferometric autocorrelation or non-collinear intensity autocorrelation.

3. Experimental results

Because the principal effect involved in ZDW fibers is self phase modulation (SPM), the SPM maximum phase-shift parameter [15] defined in Eq. (1) is a pertinent factor to scale the injected power. The phase-shift parameter is given by:

$$\Phi_{SPM} = \gamma P_0 L \quad (1)$$

where γ is the nonlinearity coefficient of the silica core, P_0 is the pulse peak power and L is the length of the fiber. We are now going to study the pulse characteristics at the output of the fiber versus this phase parameter. In order to optimize the pulse compression, we experimentally and theoretically vary this factor to look for the shortest duration of the non-collinear intensity autocorrelation. As long as $\Phi_{SPM} < 1.7\pi$ (corresponding in our case to an average power less than 40 mW) the spectrum modulations are almost exclusively due to SPM as shown in Fig. 2.

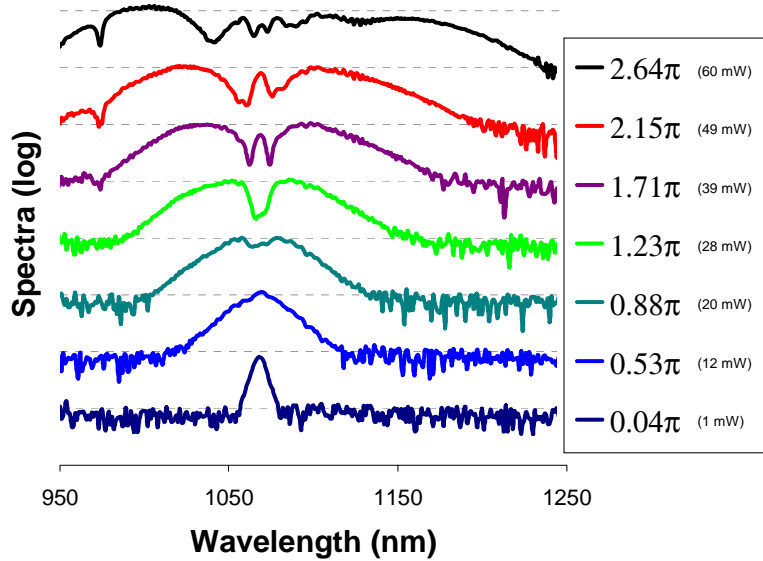


Fig. 2. Evolution of spectra versus the coupled power in the fiber (in log scale).

For higher coupled powers, third order dispersion (TOD) and self-steepening (SS) start to be perceptible as demonstrated by an asymmetry in the SPM spectrum (Fig. 3). A model based on split-step Fourier method [15] and taking into account SPM, SS and dispersion (including TOD with $\beta_3 = 0.12 \text{ ps}^3/\text{km}$) is necessary to obtain a good prediction of the non-linear processes in the microstructured fiber and of the post-compression in the prisms system.

Using this model, the optimum for compression was found near $\Phi_{SPM} = 2\pi$. In fact, as we will see in the next paragraph, for $\Phi_{SPM} > 2\pi$ the pre-pulse amplitude starts dramatically to increase and subsequently to affect the pulse temporal quality. The average power coupled in the fiber corresponding to $\Phi_{SPM} = 2\pi$ in our experiment is 47 mW. Experimentally, this optimum has been observed for a coupled power of 45 ± 2 mW. Figure 3 shows the experimental and calculated spectra for this coupled power.

The two spectra are very similar except in the shortest wavelengths region where the SPM peak is slightly more shifted toward short wavelengths for the experiment than for the theory. Thus the spectral bandwidth of these pulses is 102 nm for the experiment and only 92 nm with the model. To quantify the global difference between the spectra we used the variance defined in Eq. (2) of the two spectra $S_{exp}(\lambda)$ and $S_{theo}(\lambda)$. The variance is defined such as:

$$\Delta(f(x), g(x)) = \sqrt{\frac{1}{N} \sum_{i=1}^N (f(x_i) - g(x_i))^2} \quad (2)$$

where N is the number of point for the experimental data acquisition. Thus despite the shift of the SPM blue-peak the difference between the experiment and the theory is relatively low with $\Delta(S_{\text{exp}}(\lambda), S_{\text{theo}}(\lambda)) = 3\%$.

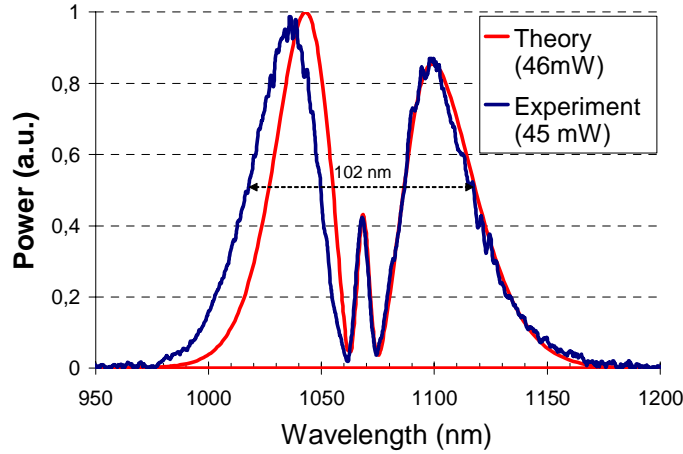


Fig. 3. Experimental and theoretical spectra (due to SPM, SS and TOD) for a coupled average power about 45 mW ($\Phi_{\text{SPM}} \approx 2\pi$).

The pulse duration of the compressed pulses has also been measured with a non-collinear autocorrelator. Figure 4 shows the experimental and calculated autocorrelation traces for a coupled power of 45 ± 2 mW.

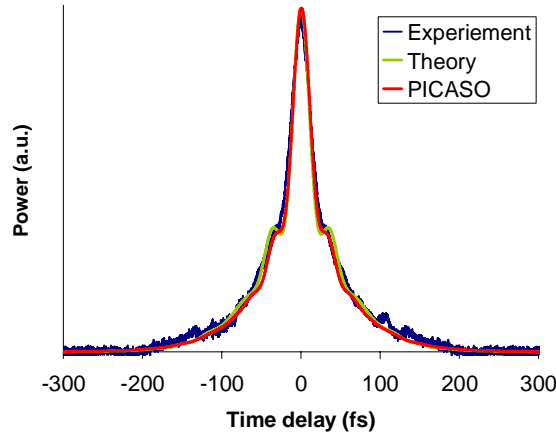


Fig. 4. Theoretical, retrieved and experimental non-collinear autocorrelation traces.

The experimental results are in good agreement with the predicted result corresponding to 46 mW of coupled power. This relatively good fitting allows the retrieving of the amplitude and phase of the pulse from the model with an accuracy of $\Delta(A_{\text{exp}}(\tau), A_{\text{theo}}(\tau)) = 1.7\%$ [16] mainly due to the background noise of the experimental autocorrelation. In this case, the

pulse duration is 21 fs and the pre-pulse amplitude is 17 % (Fig. 5) of the main maximum peak.

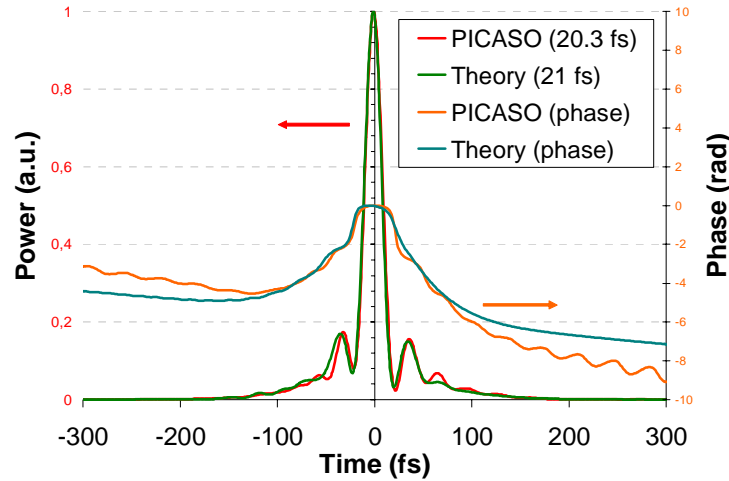


Fig. 5. Theoretical and experimental retrieved pulse shape and phase.

In order to retrieve the experimental pulse shape and duration, we used two different methods. The first one consists in fitting the interferometric autocorrelation with the model; then the retrieved pulse is given by the model. The only variable parameter used in this fit is the coupled power in the fiber. The second method used a phase retrieving based on a minimization method using the experimental spectrum (PICASO method[16]). This method is based on the minimization of the difference between the experimental and calculated correlations[10], this difference being evaluated by the factor: $\Delta(A_{\text{exp}}(\tau), A_{\text{theo}}(\tau))$. The advantages of the PICASO method compared to the interferometric autocorrelation are clear: the PICASO method includes the experimental spectrum and does not require a validation of the model. In order to avoid the problem of solution ambiguity due to the use of PICASO minimization method, we use, as initial data in the minimization process, the pulse provided by our model. Thus thanks to the relatively good agreement between our model and experiment we avoid problem of convergence. The drawback of the PICASO method is only observed when the satellite-pulse amplitudes are too important (typically >20 %) which leads to a loss of accuracy in the convergence process of the algorithm. Anyway, in our present case, the PICASO method is more accurate and precise than the interferometric autocorrelation.

The retrieved pulse and phase using PICASO are plotted in Fig. 5 and the corresponding intensity autocorrelation is plotted in Fig. 4. The retrieved pulse duration is then 20.3 fs (corresponding to 6 cycles at FWHM) for a $\Delta(A_{\text{exp}}(\tau), A_{\text{theo}}(\tau))=1.6\%$ and the pre-pulse amplitude is around 17 %. The pulse retrieved by the PICASO method and the pulse calculated from the numerical simulations are very similar validating thus the use of the model taking into account self-phase modulation, group velocity dispersion, third order dispersion and self-steepening. Moreover, the influence on the pulse duration of the non-compensated high-order dispersion (mainly TOD, SS) is far from significant (less than 1 fs) and concerning the pre-pulse amplitude the uncompensated TOD and SS leads to a relative increase from 13 % to 17 %. Some numerical simulations taking into account the stimulated Raman scattering (SRS) using the model described in reference 17 have also been done and no influence of this effect have been observed on the results for this range of incident power.

Consequently, the numerical simulations taking into account SPM, GVD, TOD and SS is sufficient to efficiently simulate the compression down to the 20 fs range. The 20 fs compressed pulses have a relatively good quality with a satellite-pulse amplitude of 17 % and

a time bandwidth product of 0.54. The average power after compression is 30 mW corresponding to a peak power of 9.3 kW.

4. Limitations

In order to put in evidence the limitations of our compression system, we studied the pulse compression for higher coupled power in the PCF. We are now confronted to important satellite pulses; then, the non-collinear intensity autocorrelations turn out to be too broad for an accurate measurement of the duration using PICASO algorithm. The use of the interferometric autocorrelation was then preferred[6], whereas it exhibits a lower precision than the PICASO method when pulse satellites have a small amplitude. Fitting the central fringes of interferometric autocorrelations (by adjusting only the coupled power in the fiber) allows then a fairly accurate estimation of the pulse duration even with relatively important pre-pulses. As shown in Fig. 7, these experimental durations are in good agreement. This good agreement has been observed until $\Phi_{SPM} < 2.5\pi$ (corresponding to average powers less than 60 mW).

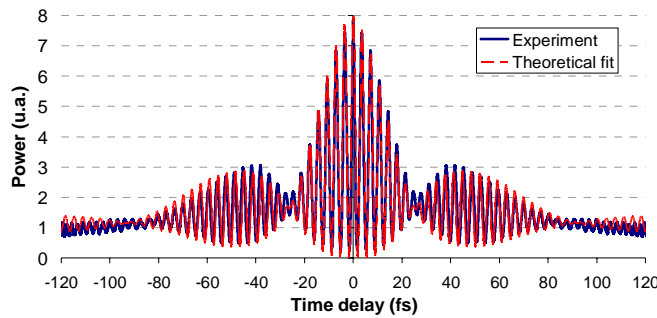


Fig. 6. Example of interferometric autocorrelations for $\Phi_{SPM} \approx 2\pi$. The fitting assuming a pulse shape given by the model allows a fairly accurate estimation of the pulse duration.

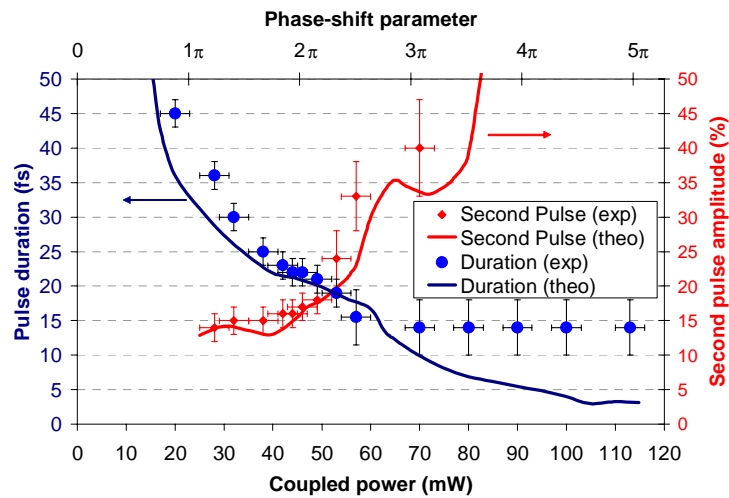


Fig. 7. Pulse duration of compressed pulses after the prism-compressor and influence of the pre-pulse amplitude.

Fitting the interferometric autocorrelation traces and using the model previously described, we also could retrieve the pre-pulse amplitude. This second pulse amplitude is plotted in Fig. 7. We observe that for a coupled power higher than 47 mW, amplitude of the

satellite pulses drastically increases. This consideration of the pulse quality gives the first limitation of our system. For pulses $2\pi < \Phi_{SPM} < 2.5\pi$ it is possible to predict, with still a relatively good accuracy, the spectral broadening (Fig. 8) and compression factor but the compression leads to pulses with intense and numerous satellite pulses.

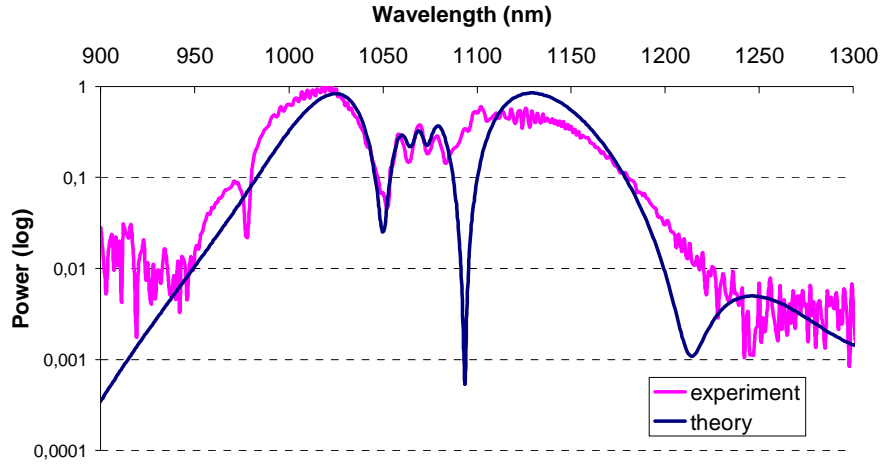


Fig. 8. Experimental and theoretical spectra for $\Phi_{SPM} \approx 2.5\pi$ (≈ 57 mW) just below the SRS splitting.

In order to visualize the evolution of the pulse compression versus the injected power in the PCF fiber, we plot spectrograms for $\Phi_{SPM} \in [0, 3\pi]$. These spectrograms[17-19] are defined as followed:

$$XFROG[E_1, E_2](\lambda, \tau) = \left| \int_{-\infty}^{\infty} E_1(t) E_2(\tau - t) e^{-i \frac{2\pi c t}{\lambda}} dt \right|^2 \quad (3)$$

where E_1 is the pulse to be analyzed, E_2 is the reference pulse considered Fourier-transform limited and defined such as : $E_2(t) = \text{sech}(1.76 t / \Delta\tau_{FWHM})$, λ is the wavelength and $\Delta\tau_{FWHM}$ is the FWHM pulse duration of P_2 . These calculated spectrograms using a reference allow a global and simple visualization of the defect of compression in the spatial and temporal domain.

The first spectrogram shows the evolution of the pulses at the output of the fiber. In order to optimize the resolution of the spectrogram we also computed the XFROG between the output pulse (E_{fiber}) and the input pulse (E_{input}), *id est* a transform limited sech^2 pulse of 110 fs. These spectrograms: $XFROG[E_{\text{fiber}}, E_{\text{input}}]$ are illustrated in the first column of Fig. 9 for $\Phi_{SPM} \in [0, 3\pi]$. This XFROG can be compared to the XFROG presented in the work of Hilligsoe and al. on super-continuum generation in PCF[19]; and it can be observed that our regime of compression is far below the super-continuum generation.

In order to demonstrate the efficiency of the compression with an adapted time scale, we plots a second chronogram that represents the XFROG between the compressed pulse ($E_{\text{compressed}}$) and an ideal transform limited sech^2 pulse with the same duration (E_{TF}). These spectrograms: $XFROG[E_{\text{compressed}}, E_{\text{TF}}]$ are illustrated in the second column of Fig. 9 for $\Phi_{SPM} \in [0, 3\pi]$. Moreover, in order to put in evidence the quality of the compression and the pedestal influence we compared this XFROG with the FROG for ideal transform limited sech^2 pulse of the same duration. These spectrograms $XFROG[E_{\text{compressed}}, E_{\text{TF}}] - XFROG[E_{\text{TF}}, E_{\text{TF}}]$ are

illustrated in the third column of Fig. 9 for $\Phi_{SPM} \in [0, 3\pi]$. The model clearly indicates that for 110-fs input pulses the influence of the pedestal limits the pulse compression in the 20 fs range e.g. to $\Phi_{SPM} \approx 2\pi$. Actually, for higher non-linear phase, the pedestal, as indicated by $\text{XFROG}[E_{\text{compressed}}, E_{\text{TF}}] - \text{XFROG}[E_{\text{TF}}, E_{\text{TF}}]$ clearly breaks up in multiple dots.

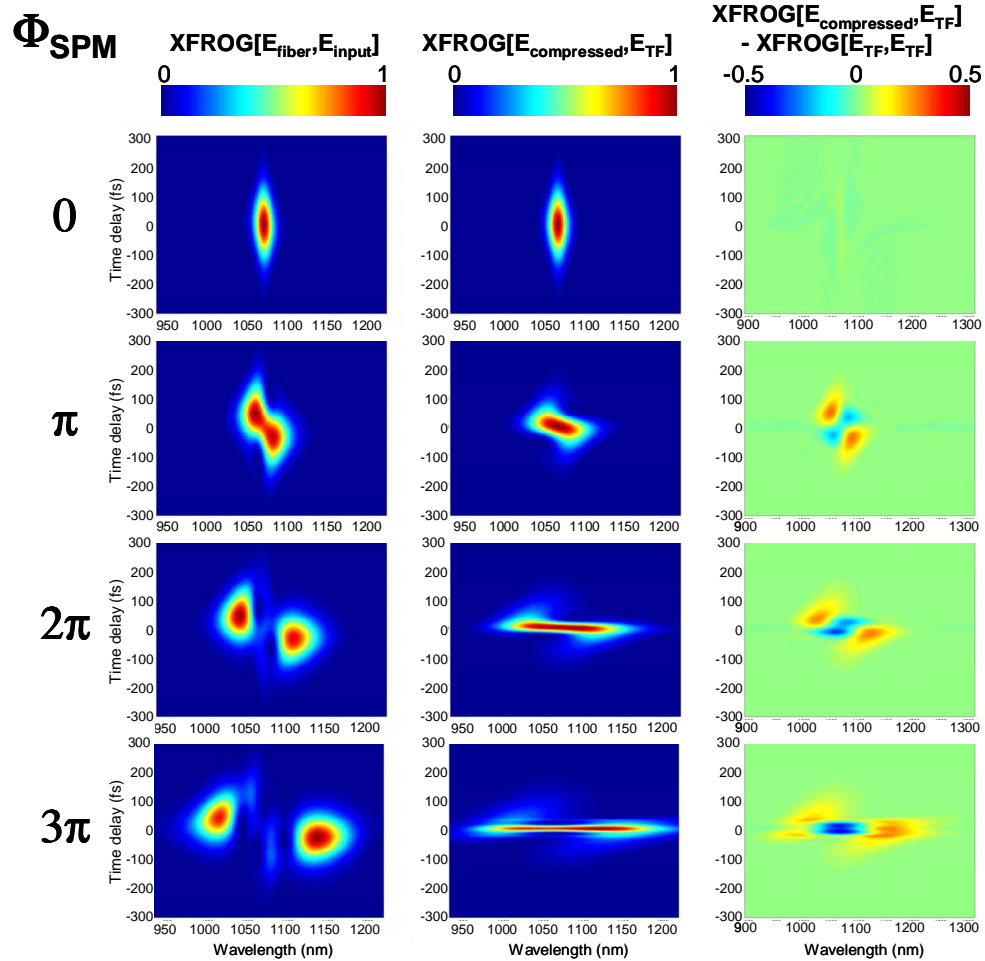


Fig. 9. XFROG traces for different non-linear phase shifts: the first column represents $\text{XFROG}[E_{\text{fiber}}, E_{\text{input}}]$ which puts the emphasis on the spectrum generation by SPM in the PCF fiber; the second column represents $\text{XFROG}[E_{\text{compressed}}, E_{\text{TF}}]$ which puts the emphasis on the compression efficiency and the third column represents $\text{XFROG}[E_{\text{compressed}}, E_{\text{TF}}] - \text{XFROG}[E_{\text{TF}}, E_{\text{TF}}]$ which puts the emphasis on the compressed-pulse quality.

To see the ultimate limitation of our compression system, we increase furthermore the coupled power in the fiber. Then, we observed that for $\Phi_{SPM} > 2.5\pi$, the central pulse duration stays relatively constant because of a soliton fission[20-22] in the fiber due to the both combined effects of soliton self-frequency shift (SSFS) by stimulated Raman scattering (SRS) and third order dispersion. This soliton fission can be observed in both spectral domain as shown in Fig. 10 and temporal domain by misaligning the distance between the prisms in the compressor. The occurrence of this soliton fission corresponds to the pulse-compression limitation as shown in Fig. 11; the pulse duration (at FWHM) of the shortest pulse is then estimated to

14 ± 4 fs using the interferometric autocorrelation -instead of ≈ 4 fs predicted by the theory without taking into account the SRS limitation. Numerical simulations taking into account the SRS and SSFS[21] has been performed and shows a Raman splitting threshold for $\Phi_{SPM} \geq 3\pi$.

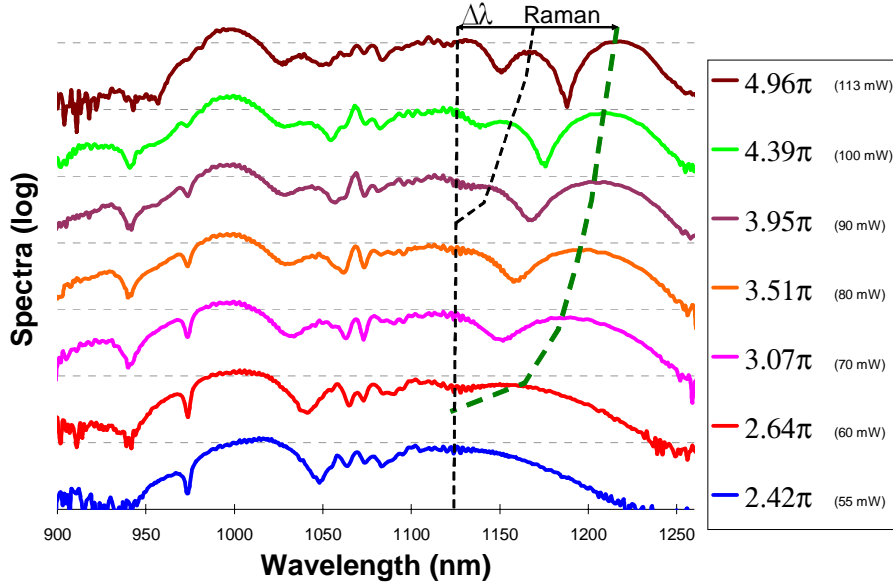


Fig. 10. Evolution of spectra versus the coupled power in the fiber (in log scale): evidence of the stimulated Raman scattering splitting and soliton self-frequency shift.

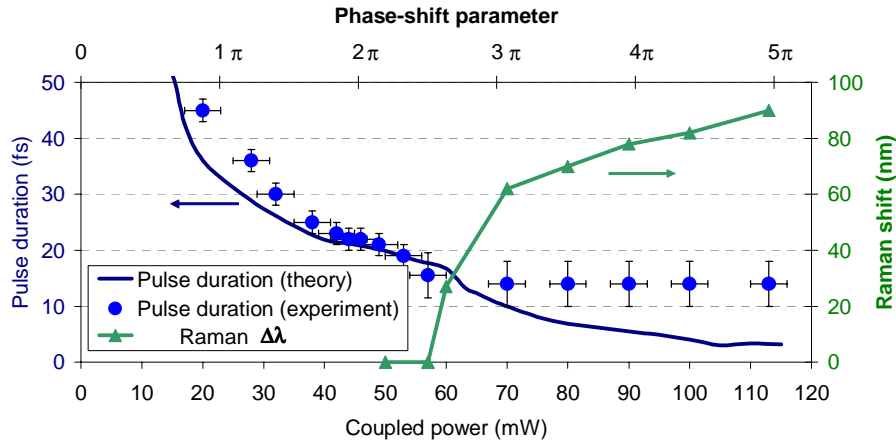


Fig. 11. Pulse duration of compressed pulses after the prism-compressor and influence of the SRS splitting see also Fig.10.

Experimentally we observed that the soliton fission is limiting the long-wavelength lobe broadness of the SPM spectrum at a maximum value of 1140 nm, avoiding thus very broad band generation for the fundamental pulse. Anyway, the use of a ZDW microstructured fiber allows a pulse compression much more efficient than using self-compression in an anomalous dispersive microstructured fiber since the soliton fission limitation occurred for broader spectra in the first case. Nevertheless, although this compression leads to very few cycle

pulses, the pulse quality is relatively poor because of intense and numerous satellite pulses in the pedestal (Fig.12).

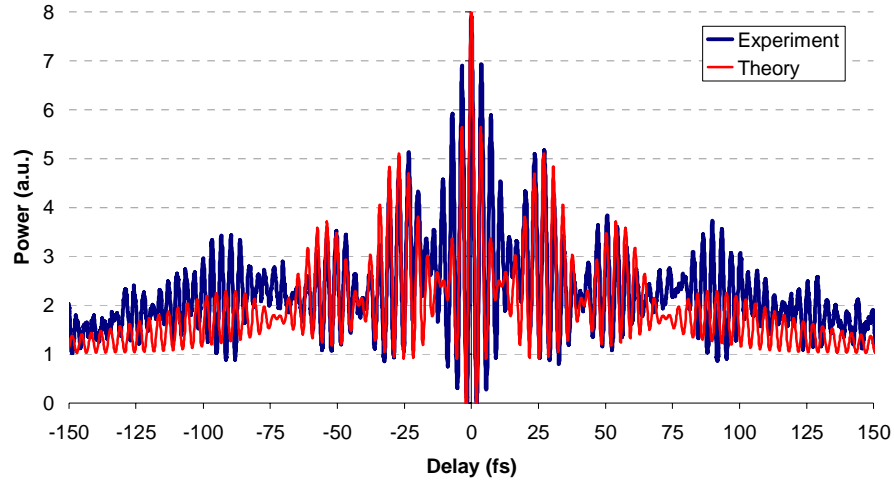


Fig. 12. Autocorrelation trace for $\Phi_{SPM} \approx 4\pi$. The experimental trace shows 7 cycles at FWHM and the theory 3 cycles both are demonstrating important satellite pulses.

In brief, we can notice first that in this range of compressed-pulse duration below 25 fs (corresponding in our case to $\Phi_{SPM} > 1.7\pi$) the optimization of the compression taking into account only SPM and GVD is not sufficient to evaluate the compression quality[11,23]. Higher order effects have then to be considered. For a compression down to 15-fs regime using a zero dispersion wavelength fiber, TOD and SS have to be taken into account and the model is in good agreement with the theory. For shorter pulse generation requiring broader spectra, SSFS by SRS needs also to be integrated in the model. Considering that in our case the limitations are mainly due the quality of the compression and not to the SRS limitation, we will now investigate the potential improvement in the compression using a ZDW PCF fiber.

5. Improvement

Knowing the accuracy of the model and the limitations for high-quality compression, it is now possible to predict and try to improve our system in the aim to product shorter pulses. The interesting parameter to be varied is the duration of pulses injected in the fiber ($\Delta\tau_i$). We set an objective of compression fixing the value of the FWHM pulse duration after compression ($\Delta\tau_f$) -for our demonstration we choose $\Delta\tau_f \in [15\text{ fs}, 20\text{ fs}, 30\text{ fs}]$ - and we investigate the quality of the compressed pulses versus the parameter $\Delta\tau_i$. For given $\Delta\tau_i$ and $\Delta\tau_f$ and considering an optimal compression, the incident average power \bar{P} is not a variable parameter anymore. It is fixed using the Eq. (4):

$$\Phi_{SPM}(\Delta\tau_i) = \gamma L \frac{\bar{P}}{F \Delta\tau_i} \approx \frac{a}{\Delta\tau_f} \Delta\tau_i - a \quad (4)$$

where F the repetition rate of the pulses, and $a = 1.6$ [15]. Assuming this condition, the spectrum generated by SPM can be then large enough for a compression down to $\Delta\tau_i$, but the compressed pulse quality strongly depends of the incident pulse duration. As an example we plot the XFROG[$E_{\text{fiber}}, E_{\text{input}}$] for 20 fs compressed pulses. This spectrogram is represented in column 1 of Fig. 13. To visualize the importance of the pulse pedestal, we plots XFROG[$E_{\text{compressed}}, E_{\text{TF}}$] (second column of Fig. 13) and

XFROG[$E_{\text{compressed}}, E_{\text{TF}}$]-XFROG[$E_{\text{TF}}, E_{\text{TF}}$] (third column of Fig. 13) for a compression down to 20 fs and versus $\Delta\tau_f$.

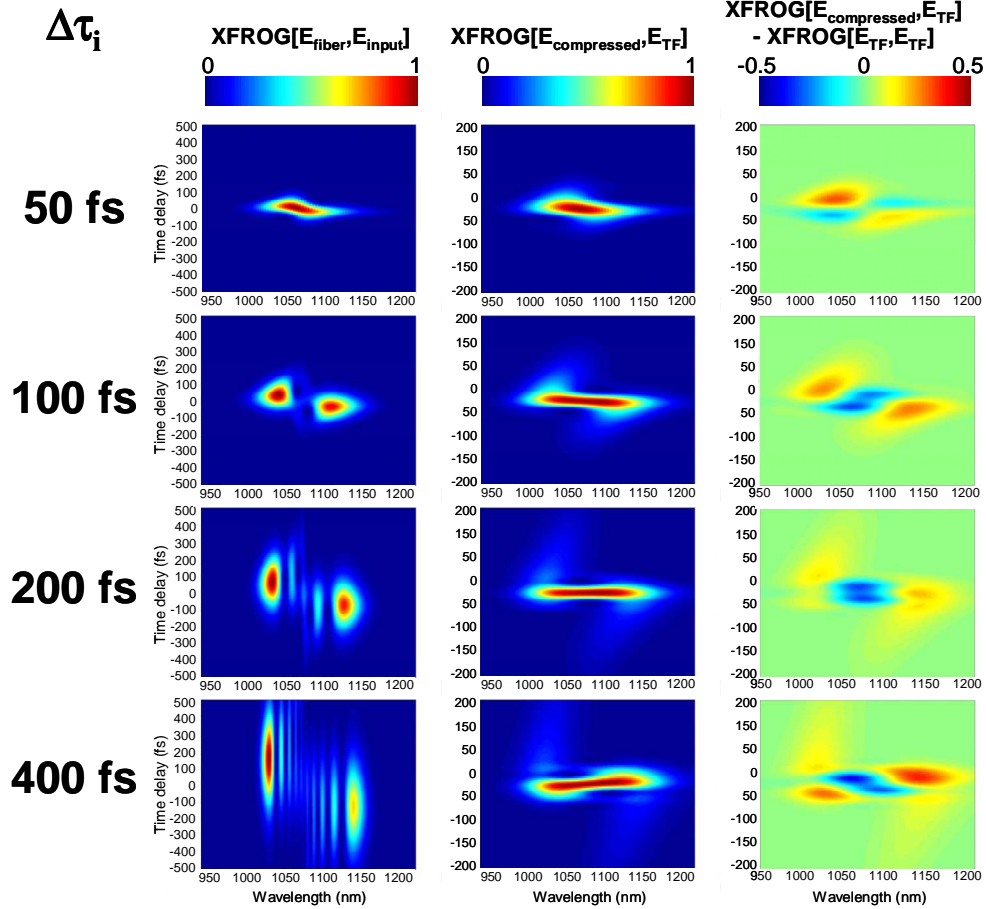


Fig. 13. XFROG traces for incident pulse duration: the first column represents XFROG[$E_{\text{fiber}}, E_{\text{input}}$] which puts the emphasis on the spectrum generation by SPM in the PCF fiber; the second column represents XFROG[$E_{\text{compressed}}, E_{\text{TF}}$] which puts the emphasis on the compression efficiency and the third column represents XFROG[$E_{\text{compressed}}, E_{\text{TF}}$]-XFROG[$E_{\text{TF}}, E_{\text{TF}}$] which puts the emphasis on the compressed-pulse quality.

It is interesting to notice that one can observe 3 different zones. In the first zone, corresponding to a very small factor of compression ($\Delta\tau_i < 100\text{ fs}$), the pulse quality really improves when the incident pulse duration decrease. In the second zone (for an incident-pulse duration between 100 fs and 200 fs) the pulse quality seems to stay relatively constant. For $\Delta\tau_i > 200\text{ fs}$ the pulse quality seems to depend again on the incident pulse duration.

In order to quantify this effect, we plot two indicators of the pulse quality which are: the second pulse amplitude (Fig. 14) and the time-bandwidth product at FWHM (Fig. 15). The second pulse amplitude corroborates the plateau between 100 fs and 200 fs already observed in the XFROG traces. But, in this region the time-bandwidth factor—which is a more global quality factor—is notably improved. In conclusion, sub-250 fs incident pulses is sufficient to obtain a compression in the 20-fs range with low amplitude satellite pulses, but working with 100-fs incident pulses allows a better transform limited pulses.

In the purpose of improving the system we also plot the same quality indicators for compressed pulses of 30 fs and 15 fs. If we limit the compression down to 30 fs, the

optimum pulse duration for the incident pulse is around 200 fs with a plateau for the secondary pulse amplitude (<15 %) between 100 and 350 fs. In the case of a compression down to 15 fs, clean compressed pulse with relatively low satellite amplitude (<20%) is not accessible for incident-pulse duration above 70 fs, which corresponds to a relatively small spectrum enlargement by SPM ($\Phi_{SPM} < 1.7\pi$). In this range of incident pulse duration, preliminary simulations including SRS seems to point out the possibility of spectrum generation leading to 10 fs compressed pulses without SSRS occurring. Future improvement in the compression using ZDW PCF fibers will then required laser oscillators producing ~50 fs pulses, which will then leads to compressed pulses in the 10-fs range.

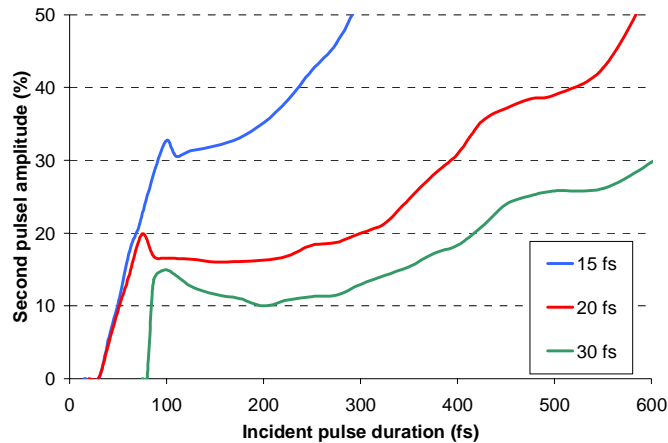


Fig. 14. Second pulse amplitude versus incident pulse duration for fixed compressed pulse durations $\Delta\tau_f \in [15\text{ fs}, 20\text{ fs}, 30\text{ fs}]$.

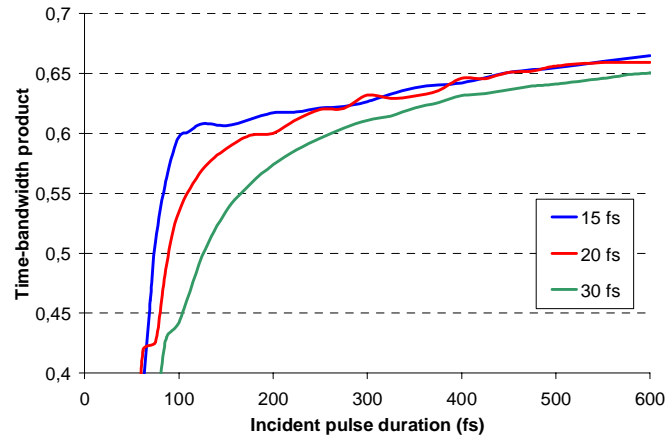


Fig. 15. Time-bandwidth product at FWHM versus incident pulse duration for fixed compressed pulse durations $\Delta\tau_f \in [15\text{ fs}, 20\text{ fs}, 30\text{ fs}]$.

6. Conclusion

In conclusion, we demonstrated pulse compression at 1 μm with the generation of very short durations based on the use of a zero dispersive wavelength photonic crystal fiber. We obtained 20.3-fs pulses with relatively low pedestal (less than 20 %), which are to our best knowledge the shortest pulses ever produced at this wavelength using a diode pumped oscillator. These experimental results can be efficiently predicted by a model including self phase modulation,

self steepening and dispersion (including third order dispersion). Moreover, shorter pulses have also been demonstrated with the production of 14-fs pulses but with important and multiple pre- and post-pulses in the pedestal. We also experimentally put in evidence the limitation of this compression technique demonstrating the emergence of soliton fission due to SRS. This simple method using ZDW PCF and prism-compressor is a very promising technique since it allows the production of ultra-short pulses within a compact system based on new efficient diode-pumped 100-fs oscillators. Using our model, we predicted the production of pulses in the 10-15 fs range with a relatively good quality by using 50 fs pulses from the oscillator. We are now looking forward to developing new diode-pumped oscillators based on Yb-doped crystal in order to proceed to the experiment.

Acknowledgments

This work has been partly support by the BIPEPSIC program from the university Paris XI.